

BLT-Based Field Coupling to Microstrip Network Model Enabling Radiated Immunity Assessment for PCB Wiring Design

Tao Liang, Yan-zhao Xie and Zhi-hao Xi
Xi'an Jiaotong University, Xi'an, China; E-mail: tao.liang@xjtu.edu.cn

Abstract

This paper proposed a statistical approach for assessing the radiated immunity of microstrip networks. For this purpose, electromagnetic field coupling to PCB is formulated by exploring the Baum-Liu-Tesche (BLT) equation, where special attention is focused on the field multi-reflections in dielectric substrate layer. Owing to the computational efficiency of deterministic model, a Monte-Carlo simulation is proposed to predict the statistical distributions and upper bound of terminal voltage across microstrip networks. The approach is then applied to compare the radiated immunity of canonical wiring layout design, which offers guidelines for improving microstrip designs.

1 Introduction

Integrated circuit (IC) is undisputedly a technology advancement milestone in modern science history, microstrip network physically connects the electronic components and chips on printed circuit board (PCB), forming up the backbones of IC circuit for reliable power and data transferring [1], [2]. However, with growing integrity density and complicity of PCB, it has become increasingly challenge to design the wiring layout with sufficient immunity due to external electromagnetic field illuminations. In this connection, this paper proposes a computational effective approach based on the Baum-Liu-Tesche (BLT) equation to assess the field coupling (FC) to microstrip network terminal responses, in particular, multi-reflection of external field on dielectric layer has been precisely accounted [3]–[5]. Accordingly, the model could be used as deterministic solution for uncertainty quantification and to predict the terminal responses of microstrip network under electromagnetic noises of random incidences. The proposed approach enables comparisons of different microstrip network in terms of radiated immunity, the obtained conclusions can be used as guidelines for PCB wiring layout design.

The paper is organized as follows: Section II summarizes the deterministic solution of FC to arbitrary microstrip network by exploiting the BLT equation and field reflection in multi-layer media. Section III demonstrates the MC simulation approach and compares the performance of different wiring design strategy, finally, the conclusions are drawn in Section IV.

2 Field Coupling to Microstrip Network Model

2.1 Microstrip Network under Illumination of Electromagnetic Field

This paper considers a general scenario of microstrip network illuminated by an external electromagnetic field. As shown in Figure 1, the three-layer PCB of length b and width a is placed on the x - y plane, the network is excited by a plane field of magnitude E^{inc} and propagation constant k_0 , the electric field direction is defined by polar angle θ , azimuth angle ϕ and polarization angle η . Apparently, the incidence of field is intrinsically random in practice, which is propulsion of introducing statistical analysis for wiring designs. Both trace and ground layer are assumed to be perfect electric conductor, ohmic loss is neglected, whereas, the substrate is made of dielectrics (commonly FR4) of relative permittivity ϵ_r .

For simplicity, the investigation has made the following assumptions: 1) all branches of microstrips sharing the same geometric structure, namely, trace thickness t and width w , as shown in Figure 2. Seeing the fact that t is much smaller than the substrate height h , one could neglect the impact of thickness t during the trace modeling process; 2) near-field coupling between microstrip branches are neglected [6], accordingly, single-conductor BLT equations can be applied for modeling the coupling efficiency.

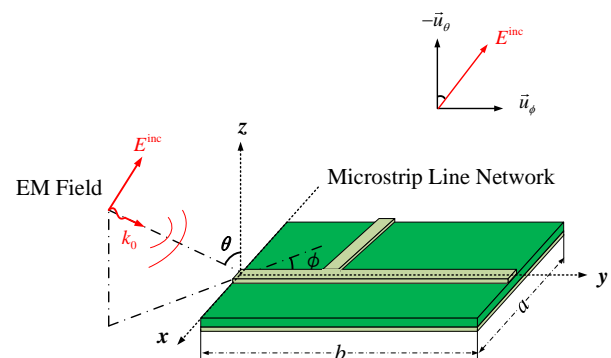


Figure 1. A PCB carrying Microstrip network under illumination of plane electromagnetic field.

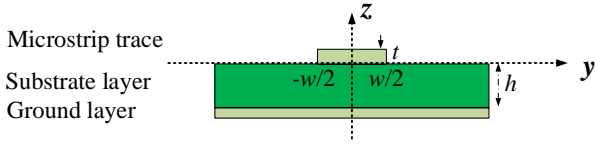


Figure 2. Microstrip cross-section (transversal view).

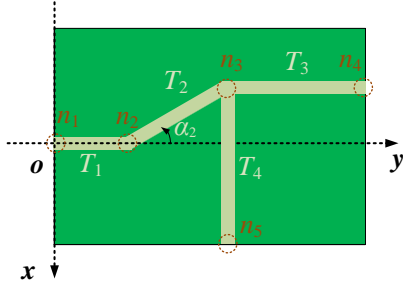


Figure 3. Microstrip wiring layout (top view).

To define layout of microstrip network, a top view of the PCB is depicted in Figure 3, in which, the straight microstrip segments are enumerated by $\{T_1, \dots, T_n\}$, which has the length of $\{l_1, \dots, l_n\}$, respectively. Angle $\{\alpha_1, \dots, \alpha_n\}$ defines the anti-clockwise rotation of segment with respect to $+y$. the terminals of lines are denoted as nodes $\{n_1, \dots, n_m\}$, where lumped impedance $\{Z_1, \dots, Z_m\}$ could be applied at nodes to as termination between trace and ground.

2.2. Deterministic Solution for Field coupling to Microstrip Network Terminal Responses

By treating the microstrips as single-conductor transmission line network, BLT equation can be used to predict the terminal load voltage (\mathbf{V}_L) and current (\mathbf{I}_L) across terminal impedances of nodes, namely, the

$$\begin{aligned} \mathbf{I}_L &= \mathbf{Z}_C^{-1}(\mathbf{U} - \boldsymbol{\rho})(-\boldsymbol{\rho} + \boldsymbol{\Gamma})^{-1}\mathbf{S}; \\ \mathbf{V}_L &= (\mathbf{U} + \boldsymbol{\rho})(-\boldsymbol{\rho} + \boldsymbol{\Gamma})^{-1}\mathbf{S}; \end{aligned} \quad (1)$$

Where \mathbf{U} is a $2n$ -by- $2n$ identity matrix, characteristic impedance \mathbf{Z}_C is a diagonal matrix, whose element can be estimated by empirical expressions or by simulation [4]. The voltage reflection matrix $\boldsymbol{\rho}$ is $2n$ -by- $2n$ diagonal matrix, where the i^{th} diagonal element is given by $(Z_i - Z_{Ci})(Z_i + Z_{Ci})^{-1}$; propagation matrix $\boldsymbol{\Gamma}$ are cast as

$$\boldsymbol{\Gamma} = \begin{bmatrix} \mathbf{O} & \mathbf{P} \\ \mathbf{P} & \mathbf{O} \end{bmatrix}, \quad (2)$$

Where \mathbf{O} is n -by- n zeros, \mathbf{P} summarizes the propagation term $e^{j\beta l_i}$ associated to i^{th} trace segment at diagonal, $\beta = k_0 \sqrt{\varepsilon_r^{\text{eff}}}$, $\varepsilon_r^{\text{eff}}$ is effective relative permittivity of the PCB [4].

The source matrix $\mathbf{S} = [\mathbf{S}_1, \mathbf{S}_2]^T$ collects active contributions of external field, according to Agrawal's model, \mathbf{S} is the summation of longitudinal (E_y) electrical field contribution (v_y^{s+} and v_y^{s-}) and terminal transversal (E_z) electrical field (v_0^s and v_l^s), that is:

$$\begin{pmatrix} \mathbf{S}_1 \\ \mathbf{S}_2 \end{pmatrix} = \frac{1}{2} \begin{pmatrix} v_0^s + v_y^{s+} - v_l^s e^{j\beta l_i} \\ \dots \\ -v_0^s e^{j\beta l_i} - v_y^{s-} e^{j\beta l_i} + v_l^s \\ \dots \end{pmatrix}, \quad i = 1, \dots, n; \quad (3)$$

Particularly, the assessment of \mathbf{S} should account for the multi-reflections of external field in the substrate layer, since both ground and trace layer could perfectly reflect the incident field. In this connection, it is necessary to further separate the incident field into decoupled TE and TM components:

$$\begin{cases} E_y^{\text{inc}} = \underbrace{E^{\text{inc}} \cos \theta \cos \phi \cos \eta}_{\text{TM component: } E_y^{\text{TM}}} + \underbrace{E^{\text{inc}} \sin \phi \sin \eta}_{\text{TE component: } E_y^{\text{TE}}} \\ E_z^{\text{inc}} = E_z^{\text{TM}} = E^{\text{inc}} \sin \theta \cos \eta \end{cases} \quad (4)$$

For the longitudinal field contribution, the resultant can be obtained by:

$$\begin{aligned} E_y &= E^{\text{inc}} e^{-jk_y y} F_y; \\ F_y &= \sin \phi \sin \eta (1 + R^{\text{TE}}) + \cos \theta \cos \phi \cos \eta (1 - R^{\text{TM}}); \end{aligned} \quad (5)$$

Where $k_y = k_0 \sin \theta \cos \phi$, F_y is function of external field and PCB architecture. The TE/TM reflection coefficients can be evaluated as function of :

$$\begin{aligned} R^{\text{TE}} &= \frac{r^{\text{TE}} - e^{-j2k_{dz}h}}{1 - r^{\text{TE}} e^{-j2k_{dz}h}}; \quad R^{\text{TM}} = \frac{r^{\text{TM}} + e^{-j2k_{dz}h}}{1 + r^{\text{TM}} e^{-j2k_{dz}h}}; \\ r^{\text{TE}} &= \frac{\cos \theta - \sqrt{\varepsilon_r - \sin^2 \theta}}{\cos \theta + \sqrt{\varepsilon_r - \sin^2 \theta}}; \\ r^{\text{TM}} &= \frac{\varepsilon_r \cos \theta - \sqrt{\varepsilon_r - \sin^2 \theta}}{\varepsilon_r \cos \theta + \sqrt{\varepsilon_r - \sin^2 \theta}}; \end{aligned} \quad (6)$$

The z -direction propagation constant inside substrate is $k_{dz} = k_0 \sqrt{\varepsilon_r - \sin^2 \theta}$. Accordingly, it is convenient to evaluate source term associated to i^{th} trace by integrating $v_y^{s+} = \int_0^{l_i} E_y(y) e^{j\beta y} dy$ and $v_y^{s-} = \int_0^{l_i} E_y(y) e^{-j\beta y} dy$, which leads to:

$$v_y^{s+} = E^{\text{inc}} F_y \frac{e^{j(\beta - k_y)l_i} - 1}{j(\beta - k_y)}; \quad v_y^{s-} = E^{\text{inc}} F_y \frac{e^{-j(\beta + k_y)l_i} - 1}{-j(\beta + k_y)}; \quad (7)$$

In the similar fashion, the transversal field contributed source terms can be obtained by:

$$v_0^s = E^{\text{inc}} F_z \frac{1 - e^{-j2k_{dz}h}}{jk_{dz}} \quad (8)$$

$$v_l^s = E^{\text{inc}} F_z \frac{1 - e^{-j2k_{dz}h}}{jk_{dz}} e^{-jk_y l} \quad (9)$$

The field-determined coefficient F_z can be evaluated by:

$$F_z = \frac{\sin \theta \cos \gamma (1 + r^{\text{TM}})}{\epsilon_r (1 + r^{\text{TM}} e^{-j2k_{dz}h})} \quad (9)$$

To this end, by substituting (7)-(9) back to (1), one could finally solve the field-induced terminal voltage/current.

2.4. Validation of the Deterministic Model

To demonstrate accuracy of the deterministic model, a Y-shape microstrip network of three segments is considered, the (x, y) position of nodes are: $n_1(0, 0)$, $n_2(0, 100 \text{ mm})$, $n_3(-60 \text{ mm}, 60 \text{ mm})$, $n_4(0, 40 \text{ mm})$, respectively. Resistors of value $R_1=50 \Omega$, $R_2=100 \Omega$ and $R_3=30 \Omega$ are terminated at node n_1 , n_2 , n_3 , respectively, whereas the interconnection node n_4 is left unterminated. In addition, PCB is designed by the following parameters: $t=35 \mu\text{m}$, $w=1 \text{ mm}$, $h=1.5 \text{ mm}$ and $\epsilon_r=4.7$. The PCB is illuminated by a plane field of normalized electrical field magnitude, that is, $E^{\text{inc}} = 1 \text{ V/m}$, without losing generality, it is assumed the incidence of impinging field follows: $\theta = 70^\circ$, $\phi = 90^\circ$ and $\eta = 45^\circ$.

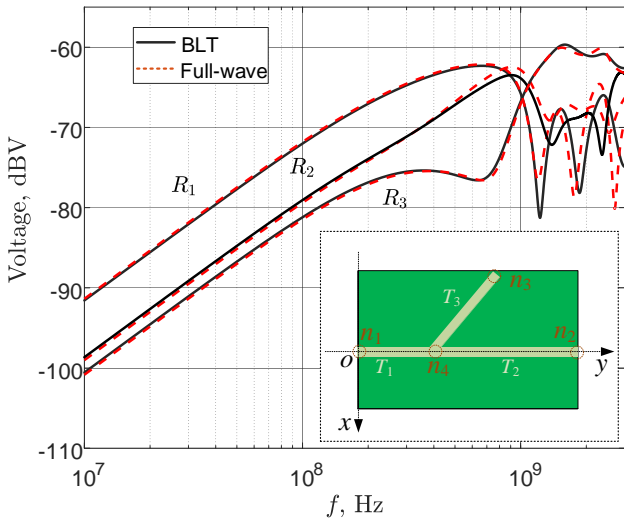


Figure 4. Comparison of field induced load voltage for microstrip network in inset by proposed BLT-based model and full-wave simulations.

Figure 4 summarized the predicted load voltages by proposed deterministic model in the bandwidth of [10 MHz, 3 GHz], the full-wave simulation result by finite integer technique is applied as benchmark, which directly solves the maxwell equation and adopts no simplifications for the

computation. From the figure, it is evident that the solutions are in good agreement, the proposed BLT-based model demonstrate good accuracy in the frequency range of interests for all three loads, discrepancies at high frequencies can be ascribed to errors due to neglect of mutual coupling between misaligned traces and high-order propagation modes. Additionally, it is worth noticing that BLT-based model is computational efficient than the full-wave solver, for this particular case, the time cost is 5 s (BLT) against 400 s (full-wave), the solid improvement of efficiency enables statistical analysis on the radiated immunity, which will be discussed in following section.

3 Statistical Analysis for Assessing Radiated Susceptibility

3.1 MC Analysis Accounting for Randomness of Field Incidence and Polarization

Owing to the excellent computational efficiency of deterministic model, brutal Monte-Carlo (MC) simulation can directly be applied to predict the statistical distribution of field induced load voltage for different wiring designs. Since there is lack of knowledge on the incidence and polarization of impinging field in practical scenarios, it is assumed the probability of incidences are equal for all direction. In the upper hemisphere, the input random variables could be sampled by:

$$\begin{aligned} \theta &= \text{acos}(1 - 2u); \quad \phi = 2\pi v; \\ \eta &\sim U[0, 2\pi]; \end{aligned} \quad (10)$$

Where axillary random variables follow uniform distributions: $u \sim U[0, 1]$; $v \sim U[0, 1]$.

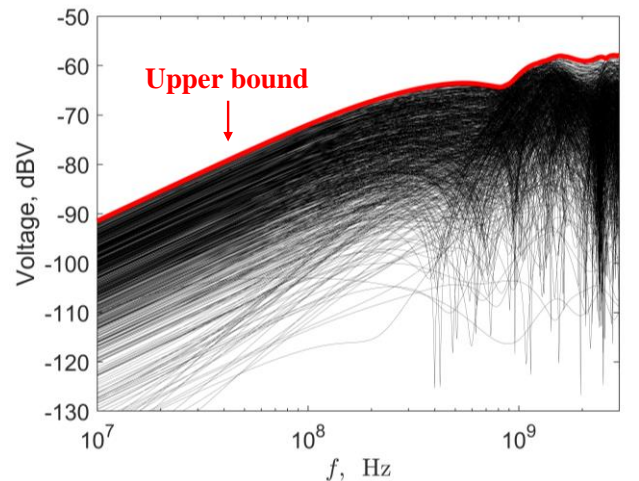


Figure 5. MC simulation of load voltage by 5000 samples to identify the upper bound.

Taking the microstrip network in Section 2.4 for case study, with 5×10^3 samples of field angles, as shown in Figure 5,

the MC analysis predicts a cluster of induced voltages spanning in a wide range. From the BLT equation, it is implied that null field-induced voltage is possible if field angles are carefully selected, conversely, the upper bound is of interest from radiated immunity viewpoint since it demonstrates the worst-case coupling scenario. Accordingly, we use upper bound as figure-of-merit to quantify the immunity of different wiring design.

3.2 Comparison of Microstrip Wiring Design by Upper Bound

(a) Microstrip Connecting two fixed terminals

Considering the simple case when two terminal loads of 50Ω locating in $(0,0)$ and $(0, 100 \text{ mm})$ need to be connected by microstrips. We compare the upper bound of load voltage for different wiring layout as shown in Figure 6. From the figure, one may notice that at low frequency (below 300 MHz), the upper bounds grow with 20 dB/dec slop and overlap with each other, there is no clear differences being identified. Conversely, with segments increase to 2 (layout #2) and 3 (layout #3 and #4), the upper bound slightly increases at high frequency range at stay at a relative stable value. By comparing results of layout #3 and #4, it is interesting to notice the cut-off frequency reduces with growth of overall trace length, therefore, for connecting fixed terminals, the optimal design is simply straight connection without any bends.

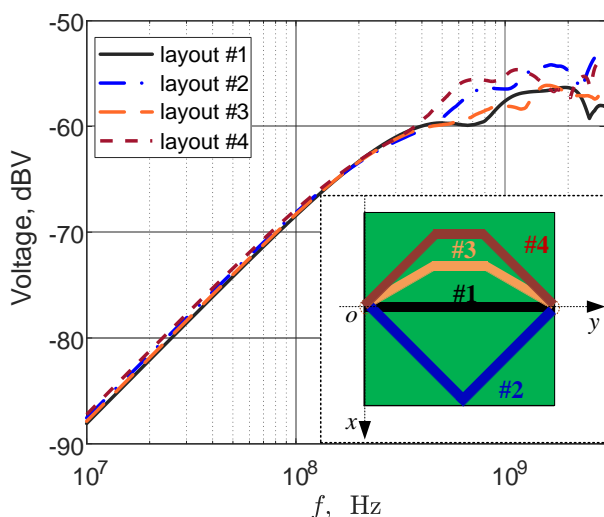


Figure 6. Comparison of load voltage upper bound for microstrips connecting two fixed terminals.

(b) Microstrip containing branches

Considering the effect of branching on radiated immunity, as shown in Figure 7, three microstrip networks are discussed, namely, straight wire (T_1+T_2), microstrip of two branches ($T_1+T_2+T_3$), and microstrip of three branches ($T_1+T_2+T_3+T_4$), the interconnection node is left open, whereas the other nodes are terminated by 50Ω . The

comparison indicates effects of branching mainly focus on low frequency. The upper bound of load voltage grows and converges gradually with increase of branch number.

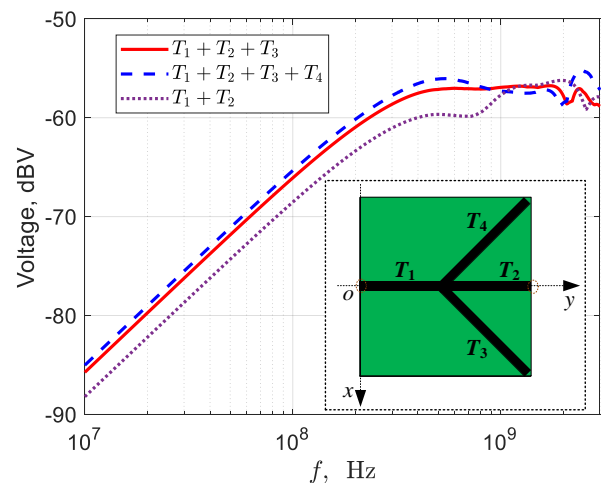


Figure 7. Comparison of load voltage upper bound for microstrips with branches.

4 Conclusions

This paper presents a radiated immunity prediction approach for microstrip networks, the approach explores the BLT equation and field reflections in multi-layer medium model, formulating a computational efficient deterministic solution to the FC problem. Accordingly, MC simulation is proposed to analyze the terminal load voltage distributions and its upper bound, which can be used as the figure-of-merit to quantify the immunity of network. Finally, case studies have been conducted to illustrate the application of proposed approach for comparing immunity performance of different wiring layout design.

References

- [1] Tzong-Lin Wu, F. Buesink, and F. Canavero, "Overview of Signal Integrity and EMC Design Technologies on PCB: Fundamentals and Latest Progress," *IEEE Trans. Electromagn. Compat.*, vol. 55, no. 4, pp. 624–638, Aug. 2013, doi: 10.1109/TEMC.2013.2257796.
- [2] S. C. Thierauf, *Understanding signal integrity*. Artech House, 2011.
- [3] F. M. Tesche, M. Ianoz, and T. Karlsson, *EMC analysis methods and computational models*. John Wiley & Sons, 1997.
- [4] M. Leone and H. L. Singer, "On the coupling of an external electromagnetic field to a printed circuit board trace," *IEEE Trans. Electromagn. Compat.*, vol. 41, no. 4 pt 2, pp. 418–424, 1999, doi: 10.1109/15.809842.
- [5] M. Mehri and A. Amini, "Stochastic EMI Noise Model of PCB Layout for Circuit-Level Analysis of System in IoT Applications," *IEEE Trans. Microw. Theory Tech.*, vol. 68, no. 12, pp. 5072–5081, 2020, doi: 10.1109/TMTT.2020.3017223.
- [6] C. R. Paul, *Analysis of multiconductor transmission lines*. New York: IEEE, 2007. doi: 10.1109/9780470547212.